Δελτίο της Ελληνικής Γεωλογικής Εταιρίας τομ. XXXX, 2007
Πρακτικά 11ου Διεθνούς Συνεδρίου, Αθήνα, Μάιος 2007

Bulletin of the Geological Society of Greece vol. XXXX, 2007
Proceedings of the 11th International Congress, Athens, May, 2007

FLUID GEOCHEMISTRY INVESTIGATIONS ON THE VOLCANIC SYSTEM OF METHANA

D'Alessandro W.[1], Brusca L.[1], Kyriakopoulos K.[2], Margaritopoulos M.[2], Michas G.[2], and Papadakis G.[2]

[1] *Istituto Nazionale di Geofisica e Vulcanologia – Sezione di Palermo, Italy*
w.dalessandro@pa.ingv.it

[2] *National and Kapodistrian University of Athens, Faculty of Geology and Geoenvironment, Department of Geology, ckiriako@geol.uoa.gr*

Abstract

An extensive geochemical survey on the fluids released by the volcanic/geothermal system of Methana was undertaken. Characterization of the gases was made on the basis of the chemical and isotopic (He and C) analysis of 14 samples. CO_2 soil gas concentration and fluxes were measured on the whole peninsula at more than 100 sampling sites. 31 samples of thermal and cold groundwaters were also sampled and analysed to characterize the geochemistry of aquifers.

Anomalies referable to the geothermal system, besides at known thermal manifestations, were also recognized at some anomalous degassing soil site and in some cold groundwater. These anomalies were always spatially correlated to the main active tectonic system of the area. The total CO_2 output of the volcanic system has been preliminary estimated in about 0.2 kg s^{-1}. Although this value is low compared to other volcanic systems, anomalous CO_2 degassing at Methana may pose gas hazard problems. Such volcanic risk, although restricted to limited areas, cannot be neglected and further studies have to be undertaken for its better assessment.

Key words: *soil gases, groundwater chemistry, CO_2 fluxes, gas hazard.*

Περίληψη

Στην ευρύτερη περιοχή του ηφαιστείου της χερσονήσου των Μεθάνων πραγματοποιήθηκε λεπτομερής ηφαιστειολογική, γεωχημική και γεωθερμική μελέτη. Τα χαρακτηριστικά των αερίων φάσεων προσδιορίστηκαν με βάση τις χημικές και ισοτοπικές αναλύσεις του He και C σε 14 δείγματα αερίων φάσεων από την περιοχή. Η συγκέντρωση και η ροή του CO_2 στην επιφάνεια του εδάφους και σε βάθος 50 εκατοστά υπολογίσθηκαν με σειρά μετρήσεων σε όλη τη χερσόνησο, σε περισσότερα από 100 σημεία δειγματοληψίας.

Αναλύθηκαν 31 δείγματα θερμών πηγών και ψυχρού επιφανειακού νερού με σκοπό να προσδιοριστούν τα ηφαιστειολογικά και γεωχημικά χαρακτηριστικά του υπογείου υδροφόρου ορίζοντα. Οι ανωμαλίες που σχετίζονται με το γεωθερμικό σύστημα, εκτός των εμφανών σημείων εκδήλωσης θερμών ατμίδων και θερμομεταλλικών πηγών, εντοπίστηκαν και σε άλλες περιοχές διαφυγής αερίων της χερσονήσου καθώς και σε ψυχρό υπόγειο νερό. Σχεδόν πάντοτε οι ανωμαλίες αυτές συνδέονται χωροταξικά άμεσα με την κύρια ενεργό τεκτονική δομή της περιοχής. Η συνολική ποσότητα CO_2

που απελευθερώνεται από το ηφαιστειακό σύστημα εκτιμάται σε 0.2 kg s^{-1}. Αν και η τιμή αυτή είναι αρκετά μικρή σε σχέση με άλλες αντίστοιχες ηφαιστειογενείς περιοχές, η ανώμαλη διαφυγή αερίων στο ηφαίστειο των Μεθάνων κυρίως CO_2, μπορεί να προκαλέσει περιορισμένους κινδύνους. Αυτά τα μετα ηφαιστειακά φαινόμενα, αν και εκδηλώνονται σε αρκετά περιορισμένες περιοχές δεν μπορεί να αγνοηθούν αλλά τουναντίον χρειάζονται επιπλέον μελέτες για την αποτίμηση του ηφαιστειακού κινδύνου.

Λέξεις κλειδιά: *Αέρια υπεδάφους, γεωχημεία υπογείου νερού, ροή CO_2, επικινδυνότητα αερίων.*

1. Introduction

Methana, a peninsula of about 44 km^2 extension at the north-eastern coast of Peloponnesus in Greece, is the westernmost dormant but geodynamically and hydrothermally active volcanic system of the South Aegean volcanic arc. The arc formed as a result of the collision between the Eurasian and Africa plates and comprises other three active volcanic systems (Milos, Santorini-Kolumbo and Nysiros), which experienced in the last centuries different kinds of volcanic activity (Pe-Piper and Piper 2002). The most recent volcanic activity on Methana dates back to 230 BC and this together with the present day thermal manifestations testifies for its potential reactivation in the future. Although the volcanic hazard of this volcanic system is considered to be low (Vougioukalakis and Fytikas 2005) it has never been studied in depth. The Saronikos gulf area, to which Methana belongs, is a neotectonic basin considered to be seismically active (Makris *et al.* 2004) and active fault systems have also been recognised on the peninsula. These tectonic lineaments are the paths for present geothermal fluid leakage and are also potential sites for magma uprise. The present work will be a contribution to the study of the geothermal fluids of the volcanic system and their relationship to the structural setting of the peninsula. A brief discussion on gas hazard problems in the studied area is also provided.

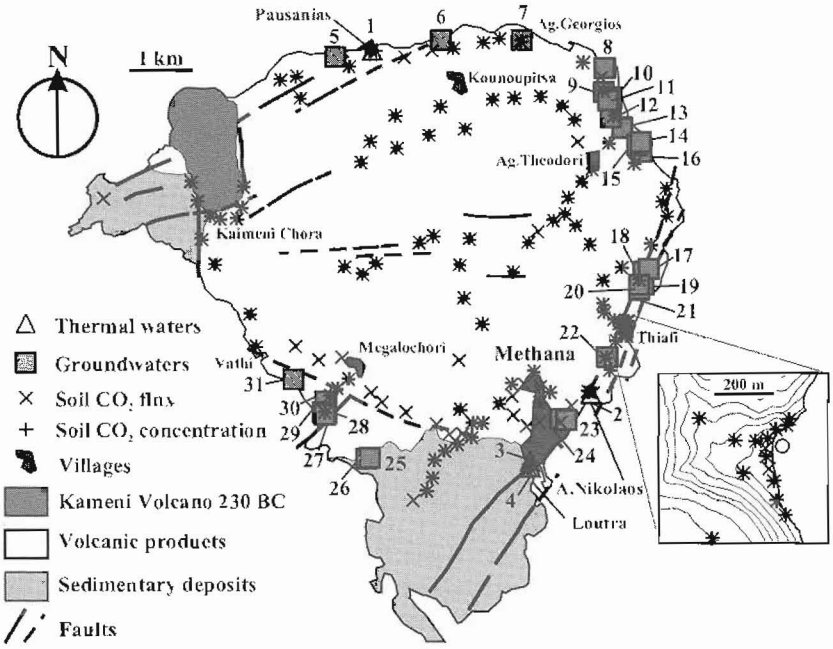

Figure 1 - Simplified geological map of Methana with the distribution of the sampling sites. Number for the water sampling points are the same as in Table 2. Inset shows the Thiafi Bay area and the circle shows the under-water sampling site of Thiafi sea (Table I)

2. Study area and methods

2.1. Geology of the area

The peninsula of Methana is almost an island, being joined to the mainland by an isthmus, which is only 300 m wide. Its otherwise almost circular outline is broken on the northwest by the projection formed by the hill of Panagia, a mass of gray limestones (U. Triassic – L. Jurassic), and on the south by the limestones of Asprovouni (U. Jurassic - Cretaceous) of which the isthmus is a prolongation (Dietrich and Gaitanakis 1995). These sedimentary sequences together form the sedimentary basement of Methana under the volcanic complex at depths not exceeding about 1000 m below sea level (Volti 1999).

The volcanic sequences of the peninsula consist principally of andesite and dacite lava domes and flows extending radially from its central part (Pe-Piper and Piper 2002). The volcanic activity probably started at the Plio-Pleistocene boundary although the oldest dated rocks gave ages of about 0.9 Ma. The most recent volcanic activity was a flank eruption that produced andesitic lavas at Kammeno Vouno around 230 BC and was described by Strabo (Stothers and Rampino 1983).

2.2. Sampling and analytical methods

In the period June - September 2006 we collected 31 samples of natural waters of Methana (Fig. 1). Four belong to thermal springs and 27 to cold groundwaters (wells). The sampled wells are all sited along the coast at distances never exceeding 200 m from the sea. They are all excavated with large diameters (1.5 – 2 m) and have depths between 1 and 30 m. The collected samples were stored in HDPE bottles. An aliquot for metal analysis was filtered in the field (0.45 μm MF Millipore filters) and acidified with HNO_3. During the same period 14 gas samples were collected, most of them are soil gases (9) but also bubbling gases (3) and the atmosphere in contact with thermal waters (2) were collected (Fig. 1). All samples were analyzed at INGV-Pa for their chemistry and He and C isotopic ratios. The temperature, pH and conductivity of waters were measured upon sampling and their alkalinity determined by titration with HCl 0.1N. Water chemistry was analysed in the laboratory by standard methods (APHA, AWWA, WEF, 1995): major anions (F, Cl and SO_4) and major cations (Na, K, Mg, Ca) by IC, Li, B and Si by ICP-OES. Theorctical CO_2 partial pressure was also calculated from measured pH, T and alkalinity. Gases were collected in pyrex bottles with two stopcocks and analyzed by gas-chromatography, using 4-m long carbosieve columns, two detectors (HWD, FID) and argon as carrier.

Helium isotopic ratio in gas samples was analyzed directly from the sampling bottles, after purification in the high-vacuum inlet line of the mass spectrometer. Helium isotope measurements were made with a VG 3000 mass spectrometer. $^3He/^4He$ ratios, determined against an air standard, are referred to the atmosphcric ratio ($Ra = 1.386\times10^{-6}$) as R/R_a. Carbon isotope analyses were performed with a Finnigan MAT Delta S mass spectrometer, after purification of CO_2 under vacuum. $^{13}C/^{12}C$ ratios are reported as $\delta^{13}C$ units (±0.1 ‰) with respect to V-PDB standard.

A total nuunber of 129 diffuse CO_2 flux measurements were made in the period 4 – 25 June 2006. The distribution of the sampling points (Fig. 1) was as far as possible evenly distributed with an approximatcly sample density of 2 points per km^2. Only few limited areas resulted uncovered due to accessibility problems. The area around the hydrothermal manifestations of Thiafi Bay was investigated with a higher sample density (13 points over an area of about 0.1 km^2). Flux measurements were made with a portable CO_2 soil flux meter (WEST Systems, Italy) based on the accumulation chamber method (Chiodini *et al.* 1998). Flux values (g m^{-2} d^{-1}) were determined at each site from the rate of CO_2 concentration increase in the chamber (area 0.031 m^2, volume 0.003 m^3) accounting for atmospheric pressure and temperature values to convert volumetric to mass concentrations. The reproducibility was better than 10% in the range 10–20000 g m^{-2} d^{-1}. Particular care was taken to fulfil the recommendations for measurements in volcanic-hydrothermal environments reported by Lewicki *et al.* (2005).

The CO_2 concentration in soil gas was measured in the field with IR spectrometry in most of the flux measurement sites (104 samples – Fig. 1). Soil gases were sampled with a syringe at a depth of 50 cm through a Teflon tube of 5 mm ID within 1 m distance from the flux measurement point. Gases were injected in the IR cell through a three-way valve. Carbon dioxide concentrations were determined with an LFG 20 (ADC Co Ltd) instrument with a 0–1000 mmol mol^{-1} range. Comparison with the results of gas-chromatographic analyses reveals a good agreement with differences never exceeding 10 %.

Table 1 – Chemical and isotopic composition of gas samples of Methana

sample	Type	He	H_2	O_2	N_2	CO	CH_4	CO_2	$\delta^{13}C$	R/R_a	He/Ne	R/R_ac
		mmol mol^{-1}							‰			
Loutra Methana	A	0.012	<0.005	54.3	313	0.0008	0.0045	642	-0.9	n.m.	n.m.	
Agios Nicolaos	A	0.008	<0.005	153	637	0.0017	<0.0005	212	-1.1	n.m.	n.m.	
Pausanias	B	<0.005	<0.005	<0.4	10.7	0.0016	0.026	991	n.m.	n.m.	n.m.	
Pausanias	B	0.0005	<0.005	5.6	30.9	0.0017	0.017	970	-2.0	2.06±0.06	2.43	2.22
Pausanias fracture	S	0.013	0.007	88.1	383	0.0580	0.0035	519	-3.5	n.m.	n.m.	
Pausanias mofette	S	0.027	<0.005	61.3	261	0.0020	0.0012	671	-2.0	n.m.	n.m.	
Soil gas 20	S	0.008	<0.005	156	642	0.0023	0.0021	203	-6.2	n.m.	n.m.	
Soil gas 21	S	0.008	<0.005	140	570	0.0020	<0.0005	293	-0.1	n.m.	n.m.	
Soil gas 23	S	0.006	<0.005	192	785	0.0018	0.0005	21.0	-8.3	n.m.	n.m.	
Soil gas 45	S	<0.005	0.082	172	704	0.0027	0.010	118	0.8	n.m.	n.m.	
Soil gas 46	S	0.0005	0.106	0.2	4.9	0.0017	0.042	966	-1.0	2.34±0.03	3.42	2.48
Thiafi	S	0.012	<0.005	51.1	266	<0.0005	0.006	675	-0.6	2.07±0.01	3.25	2.18
Thiafi	S	0.011	0.143	14.4	87.6	0.0020	0.456	881	-1.4	n.m.	n.m.	
Thiafi Sea	B	0.020	0.029	6.7	42.2	0.0090	0.717	942	-0.8	2.55±0.02	21.7	2.57

Type: A = atmosphere in contact with thermal water; B = gas bubbling in water; S = soil gas. n.m. = not measured

3. Results and Discussion

3.1. Gases

The 14 samples for which a complete analysis is available (Table 1) define a mixing trend between a CO_2 rich end-member (sample MET 46) of likely endogenous origin and the atmospheric air. This is particularly evident in the N_2-O_2-CO_2 triangular diagram (Fig. 2a), while in the He-N_2-CO_2 triangular diagram (Fig. 2b) some of the samples deviate from the simple mixing line. These samples display relative He and N_2 enrichments probably due to CO_2 dissolution processes upon interaction with seawater. The deep end-member has a typical hydrothermal gas composition being almost exclusively composed of CO_2 with minor amounts of reduced species such as CH_4, CO, H_2 and probably H_2S. This latter species was not determined but its presence, at least at Thiafi Bay, is evidenced by its smell and by fresh sulphur deposition.

The He isotopic compositions, corrected for air contamination, range from 2.18 to 2.57 R/R_a indicating a substantial contribution from a mantle component. The latter can be estimated in 34-40 % considering a composition of 8 R/R_a of the He of the mantle end-member. The carbon isotopic composition range from -8.2 to 0.8 ‰ vs. V-PDB, but a much narrower range (-2.0 to -0.8 ‰) is defined by the less air-contaminated samples (CO_2 > 880 mmol mol^{-1}). These latter values

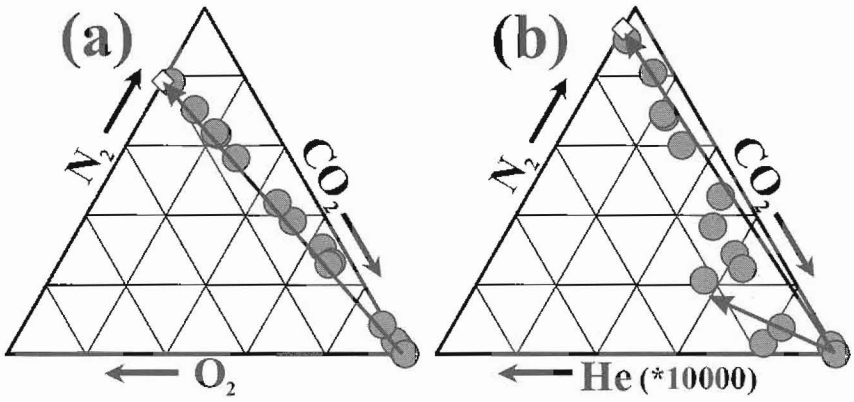

Figure 2 – N_2-O_2-CO_2 (a) and He-N_2-CO_2 (b) triangular diagrams of the gas samples collected on Methana

fall within the range generally attributed chemical or thermal decarbonation of limestones but a contribution of mantle-derived CO_2 cannot be ruled out.

Geothermometric calculations based on equilibria between carbon gases (Chiodini and Cioni 1989) gave estimated temperatures in the geothermal reservoir of 251±22 °C.

The complete set of soil gases display values from 0.2 to 966 mmol mol^{-1} of CO_2. The probability plot (Fig. 3a) evidences two lognormal distributed populations. The first population, which can be defined as background, comprises about 88 % of the measurements and displays a geometric mean of 2.45 mmol mol^{-1}, while the second "anomalous" population has a geometric mean of 206 mmol mol^{-1}. Anomalous concentrations were always measured close to active thermal manifestations (Thiafi Bay and Ag. Nicolaos and Pausanias springs - Fig. 4a).

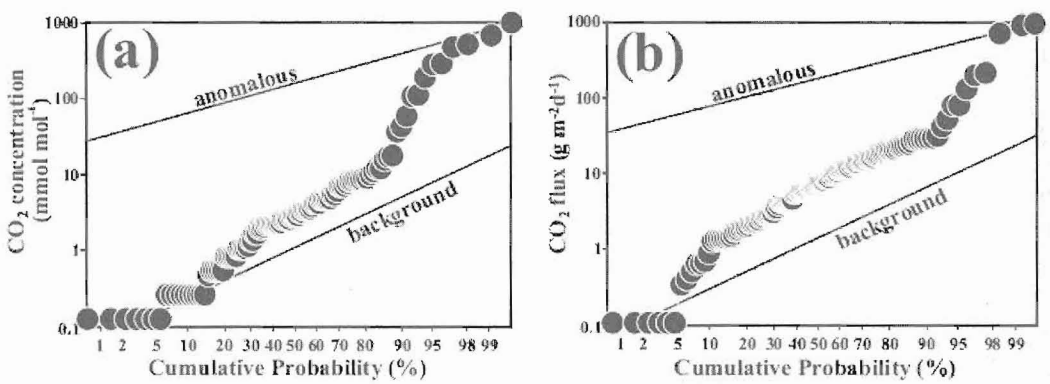

Figure 3 - Probability plot of CO_2 concentrations (a) and CO_2 flux values (b)

3.2. CO_2 fluxes

Measured CO_2 flux values range from lower detection limit (0.1) up to 894 g m^{-2} d^{-1}. Also for the flux values the probability plot (Fig. 3b) evidences two lognormal distributed populations. The background population comprises about 91 % of the measurements and displays a geometric mean of 4.75 g m^{-2} d^{-1}, while the "anomalous" population has a geometric mean of 174 g m^{-2} d^{-1}. The background population can be attributed to organic activity within the soil and its highest value (28 g m^{-2} d^{-1}) is close to the upper limit (38 g m^{-2} d^{-1}) attributed to the organic sustained CO_2 flux from the soils in the scientific literature (Norman *et al.* 1992). The values displayed by the

anomalous population are lower than at other volcanic/geothermal areas where values up to two orders of magnitude higher can be found. Chiodini *et al.* (1998) for example found CO_2 fluxes up to 11100 g m^{-2} d^{-1} at Nea Kameni volcano (Santorini, Greece) while D'Alessandro *et al.* (2006) up to 33400 g m^{-2} d^{-1} at the Sousaki geothermal area (Corinthia, Greece). Almost all the anomalous values at Methana are measured close to active thermal manifestations (Thiafi Bay and Ag. Nicolaos spring – Fig. 4b). Due to operational difficulties no flux measurement could be done close to the Pausanias spring where high soil CO_2 concentrations were measured.

The total output of CO_2 degassed from the soil of the surveyed areas was estimated using the anomaly threshold approach. Through ordinary kriging an isoflux map of the island was obtained. The CO_2 output from the anomalous population was estimated multiplying its geometric mean (174 g m^{-2} d^{-1}) by the surface (about 0.1 km^2) covered by the anomalous values (> 28 g m^{-2} d^{-1}). The obtained value, 0.2 kg s^{-1}, is at the lower end of the values measured in volcanic/hydrothermal areas (Pecoraino *et al.* 2005), but in the range of the other volcanic areas of the south Aegean volcanic arc (Nea Kameni 0.2 kg s^{-1} - Chiodini *et al.* 1998; Sousaki 0.6 kg s^{-1} - D'Alessandro *et al.* 2006; 1.0 kg s^{-1} - Cardellini *et al.* 2003).

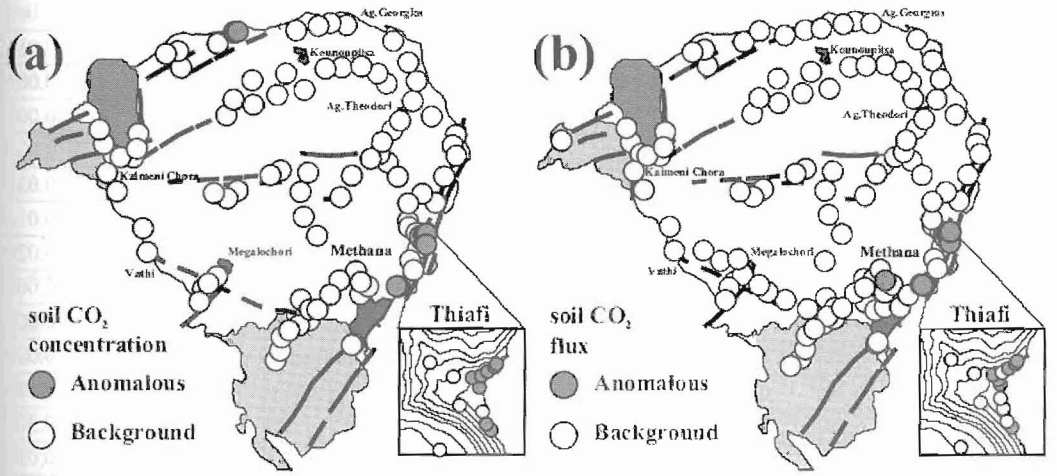

Figure 4 - Distribution of the CO_2 concentrations (a) and CO_2 flux (b) measurement sites

3.3. Thermal and cold groundwaters

The results of the chemical analysis of thermal and cold groundwaters are shown in table 2. Thermal waters have temperatures ranging between 30.5 and 37.5 °C and total dissolved solids (TDS) ranging from 10000 to 38000 mg l^{-1}. Cold waters have distinct lower temperatures (17.0-24.4 °C) and salinities (TDS 640-6200 mg l^{-1}). The influence of seawater on both thermal and cold groundwaters can be highlighted in the Na vs. Cl"binary diagram (Fig. 5a) where nearly all samples plot on the line representing the Na/Cl ratio of the Aegean seawater. Such influence can be due either to seawater intrusion both in thermal and in the cold aquifer or through the meteoric recharge. The first case is probably true for tbe waters displaying the highest salinity while for the most diluted ones the second process is more likely. The strong influence of seawater on the thermal water chemistry makes them unsuitable for geothermometric estimates of the reservoir temperatures tbrough their cationic ratios. The silica geothermometer (Nicholson 1993) gave maximum estimated temperatures of about 160 °C.

Like other volcanic/hydrothermal systems Methana's groundwaters displays high CO_2 partial pressure (pCO_2) whose values range from 0.003 to 1.138 atm thus evidencing dissolution of gases of deep origin (magma or decarbonation); groundwaters having dissolved significant amounts of magma-derived volatiles have generally pCO_2 largely exceeding the atmospheric (0.00033 atm) or soil air (0.01-0.001 atm) figures. The high pCO_2 values are faced also by high alkalinity values

(Fig. 5b) of the waters due to the titration of the dissolved CO_2 during water-rock interaction processes. Such processes are also responsible for the cation/chloride ratios higher than that of sea-water for Ca (Fig. 5c), K, B (Fig. 5d) and Li. These enrichments reveal small but significant contributions of thermalised waters to some of the cold groundwaters as highlighted by their increased content of B, a highly mobile element under geothermal conditions (Nicholson 1993).

Table 2 – Chemical composition of thermal and cold groundwaters of Methana.

sample	T	pH	E.C.	Na	K	Mg	Ca	Cl	SO_4	Alk	SiO_2	Li	B	pCO_2
N.	°C		mS cm^{-1}	mg l^{-1}								µg l^{-1}		atm
1	30.9	6.11	32.4	11028	406	1206	1009	20503	2457	1385	74.5	671	7842	1.138
2	37.5	6.32	10.2	2669	136	341	464	4686	745	1232	134	576	2985	0.624
3	30.5	6.16	26.9	5669	277	614	558	10376	1308	942	76.3	927	5557	0.690
4	30.9	6.13	50.5	11582	541	1253	1032	21442	2721	1098	48.6	1728	11470	0.861
5	26.0	7.35	2.83	492	30.1	87.2	83.8	900	101	354	89.2	76.6	434	0.017
6	22.0	7.32	2.17	356	30.9	66.6	134	712	172	238	68.8	1.7	215	0.012
7	21.0	6.98	2.11	255	12.9	114	114	517	75.4	610	79.9	6.9	157	0.068
8	19.1	7.27	2.34	389	21.9	71.9	82.6	748	97.0	250	77.9	36.1	196	0.014
9	18.0	8.10	2.15	252	13.3	53.3	83.8	448	72.5	311	75.3	45.8	161	0.003
10	21.6	7.83	2.53	530	21.1	77.8	134	782	279	500	82.0	52.9	176	0.008
11	22.5	7.15	2.10	338	14.1	79.8	110	661	98.4	351	83.8	53.2	172	0.026
12	20.2	7.19	1.98	274	14.1	89.7	97.2	542	67.7	506	91.8	53.8	162	0.035
13	17.0	7.31	1.37	143	15.6	53.9	85.8	277	109	275	81.5	4.2	81.3	0.014
14	20.3	6.80	7.80	1281	72.3	192	146	2373	399	174	69.4	4.6	486	0.029
15	18.7	7.51	1.44	189	16.0	40.2	113	399	106	232	54.6	4.6	114	0.008
16	18.3	7.49	1.17	168	10.6	40.5	74.7	327	59.5	232	80.4	17.3	84.3	0.008
17	18.5	6.98	1.60	217	17.6	44.7	152	343	48.0	613	69.7	10.9	279	0.068
18	16.5	6.30	0.73	49.9	21.1	20.9	66.3	53.5	35.5	326	34.6	5.9	162	0.173
19	20.3	6.59	4.11	688	73.5	147	219	1234	55.2	1129	98.6	365	3257	0.307
20	22.2	7.26	4.32	971	53.2	225	178	2218	22.1	421	113	176	2576	0.024
21	21.6	8.06	4.66	1067	117	199	273	2044	11.0	1214	86.0	582	4995	0.011
22	24.4	7.04	5.84	1441	41.8	247	424	3067	380	592	101	104	808	0.057
23	22.5	6.10	1.63	203	25.0	60.3	172	270	101	726	99.1	45.0	1544	0.610
24	22.2	5.95	1.46	169	22.3	36.0	118	200	107	360	103	34.8	612	0.427
25	18.9	7.02	1.63	237	9.4	37.1	138	484	73.0	299	32.9	0.98	111	0.030
26	20.5	7.60	2.84	492	12.9	63.3	183	988	145	299	31.9	0.95	166	0.008
27	21.5	6.32	3.54	701	37.9	178	259	1347	195	997	95.7	102	468	0.505
28	18.1	6.44	5.21	863	37.9	182	277	1670	257	793	77.1	38.1	447	0.305
29	21.1	6.95	2.66	411	25.8	145	236	776	109	1049	110	114	359	0.125
30	21.8	6.36	2.40	320	19.2	115	201	694	115	750	105	51.2	260	0.347
31	21.0	6.60	1.17	137	6.3	35.0	102	225	108	299	88.3	3.6	113	0.079

The highest pCO_2 valnes (Fig. 6a) and B/Cl ratios (Fig. 6b) are displayed by the thermal waters and by cold groundwaters close to them. Also samples taken south-west to Megalochori display anomalous values.

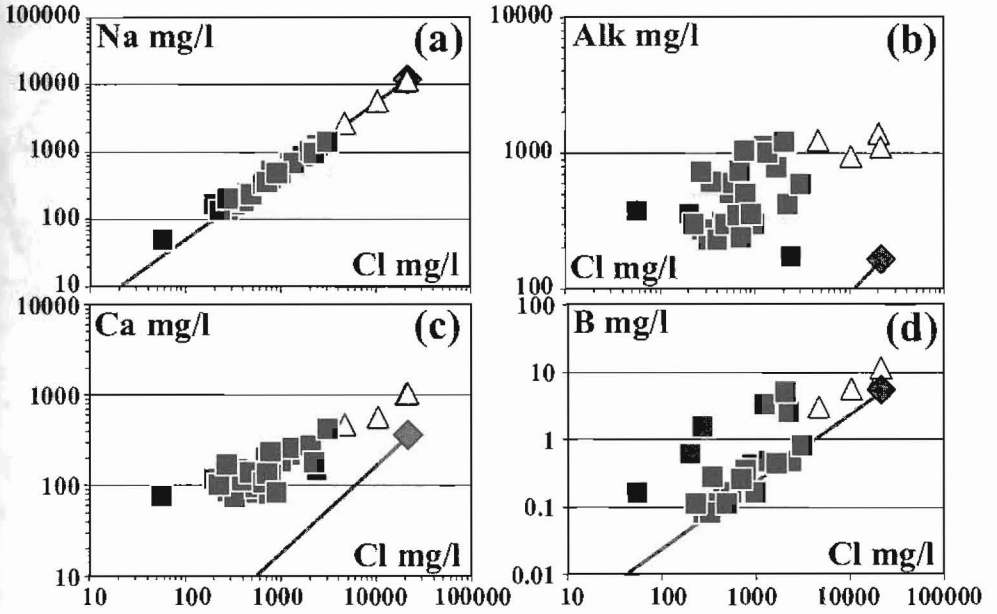

Figure 5 - Na (a), Alkalinity (b), Ca (c) and B (d) vs. chloride scatter diagrams for the groundwaters of Methana. The composition of the thermal waters is represented by triangles, that of cold groundwaters by squares and that of the Aegean seawater by a diamond. The grey bold line represents the ion/chloride ratio of the Aegean seawater

3.4. Relationships between geochemical anomalies and structural setting

The area around Methana was characterized in recent times by extensional tectonic (Makris *et al.* 2004). In the geological map of Methana (Dietrich and Gaitanakis 1995) the authors evidence many fault systems. The major Holocene systems have SW-NE (approx. 45°-60°), W-E (approx. 90°) and N-S (approx. 165°-180°) directions. Other major systems, active during Plieistocene and reactivated during Holocene have WNW-ESE (approx. 110°-135°), NW-SE (approx. 145°-150°) and SSW-NNE (approx. 25°-50°) directions. Makris *et al.* (2004), through microseismicity studies of the Saronikos gulf, attribute most of the seismic activity in the area to W-E and SW-NE tectonic structures.

Most of the geothermal manifestations on Methana (Loutra Methana, Agios Nikolaos spring and Thiafi Bay) are closely related to a SSW-NNE fault system that borders the eastern coast of the peninsula for approximately 10 km. Along the same fault system some hydrothermally altered zone, like that of Kokkinopetra, can be recognized highlighting a long hydrothermal history. The other important geothermal manifestation, Pausanias spring on the northern coast, is found along a WNW-ESE fault system. Also this system can be related to other hydrothermally altered zones and probably to the historical volcanic activity of Kammeno Vouno.

Anomalous soil CO_2 fluxes and concentrations on Methana are always found along these two fault systems further testifying for their activity (Fig 4). These anomalies, except for that of Thiafi Bay that extends for about 0.1 km^2, are always very limited in extension and very close to the hydrothermal manifestations. Our sampling density was not able to reveal other anomalies along these and other fault systems. But data from groundwaters, integrating contributions over wider areas, extend areally these anomalies along these fault systems (Fig. 6) and evidence a third anomalous area SW of Megalochori along a SW-NE directed fault and its probable intersection with a WNW-ESE directed one.

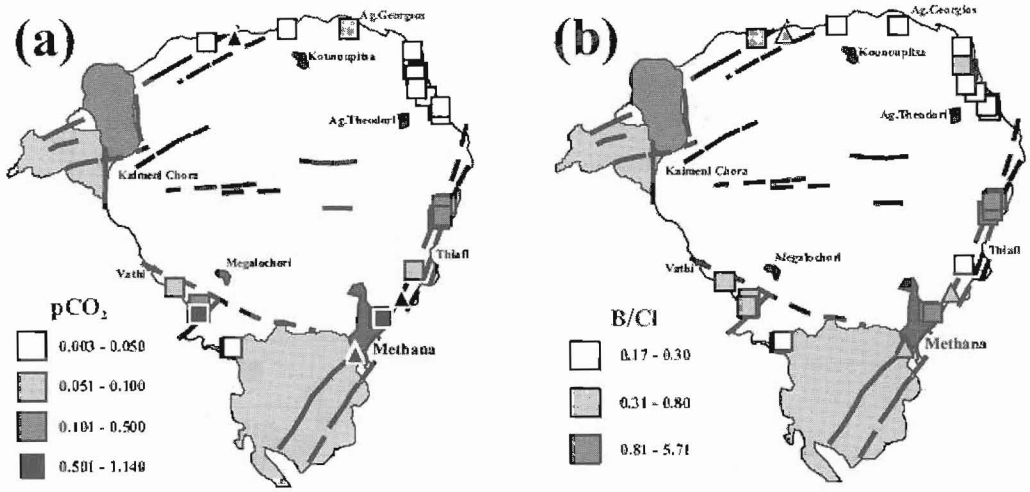

Figure 6 - Distribution of the pCO_2 (a) and B/Cl (b) values in the groundwaters

3.5. Gas hazard

Further studies have to focus on these fault systems through higher density soil gas measurements to highlight the probable presence of other anomalous degassing areas. This, apart from contributing to a better definition of the total CO_2 output of the system, could also bring to better constrain the zones of gas hazard.

Normal CO_2 concentration in the atmosphere at sea level is about 0.035 mmol mol^{-1} but its concentration can rise if fluxes from the soil exceed consumption and dissipation. Being heavier than air, in high flux areas, CO_2 can accumulate in topographic depressions and enclosures reaching concentrations as high as 100 % (1000 mmol mol^{-1}). Carbon dioxide concentrations higher than 10 % can be lethal to humans and animals, and at concentrations above 20-30 % even a few breaths can very quickly lead to unconsciousness and death from acute hypoxia, severe acidosis and respiratory paralysis (Henderson and Haggard 1943). Therefore, poorly ventilated places below and immediately above ground such as caves, galleries, trenches, cellars, water wells, etc. can be very dangerous in areas of anomalous CO_2 emissions.

Some zone of enhanced gas hazard has already been assessed also at Methana. Hazardous CO_2 accumulations have been measured at the Agios Nikolaos spring and in the well n. 23. These sites display concentrations as high as 20 % in closed spaces where sometimes persons have to work inside. Also the Pausanias spring sometimes display CO_2 concentrations of a few percent in the atmosphere at the contact with the water, but very dangerous concentrations (up to 80 %) are measured in a hole in ground some 20 m east of the spring. This hole, about 1.5 m deep and 1 m in diameter, was probably built in the past to intercept the thermal aquifer. It is at present dry, probably because of the uplift of the peninsula that led to the lowering of the piezometric surface below its bottom that is always covered by dead small animals (insects, small rodents and reptiles). The hole is fortunately not easily accessible.

People living in anomalous degassing areas are generally aware of the danger posed by gas accumulation, but nevertheless many fatal incidents due to volcanic gases happen each year (Witham 2005). Even though at Methana gas hazard seems restricted to limited areas it has not to be neglected. The most exposed people are kids, workers involved in excavation activities and tourists that use public baths.

4. Summary

At Methana the uprise of geothermal fluids is strongly controlled by the structural setting of the peninsula. Apart from the major thermal manifestations, also the major soil degassing areas and geochemical anomalies in groundwaters are found along the major fault systems of the area.

Preliminary geothermometric estimates based on carbon gas equilibria gave temperatures in the reservoir of 251±22 °C.

Soil CO_2 flux measurements ranging from 0.1 to 894 g m^{-2} d^{-1} allowed us to make a first estimation of the total CO_2 output of the volcanic/geothermal system, which was quantified in about 0.2 kg s^{-1}.

The most exhaling areas are prone to gas hazard problems and should be better studied to reduce the risk.

5. References

APHA, AWWA, WEF, 1995. *Standard methods for the determination of water and wastewater*, (Eaton A.D., Clesceri L.S. and Greenberg A.E. eds.) 19th edition.

Cardellini, C., Chiodini, G., and Frondini, F., 2003. Application of stochastic simulation to CO_2 flux from soil: Mapping and quantification of gas release, *J. Geophys. Res.* 108(B9), 2425, doi: 10.1029/2002JB002165

Chiodini, G., and Cioni, R., 1989. Gas geobarometry for hydrothermal systems and its application to some Italian geothermal areas, *Appl. Geochem.*, 4, 465-472.

Chiodini, G., Cioni, R., Guidi, M., Raco, B., and Marini, L., 1998. Soil CO_2 flux measurements in volcanic and geothermal areas, *Appl. Geochem.*, 13, 543-552.

D'Alessandro, W., Brusca, L., Kyriakopoulos, K., Rotolo, S., Michas, G., Minio, M., and Papadakis, G., 2006. Diffuse and focused carbon dioxide and methane emissions from the Sousaki geothermal system, Greece, *Geophys. Res. Lett.*, 33, L05307.

Dietrich, V., and Gaitanakis, P., 1995. Geological map of Methana peninsula (Greece), ETH Zürich, Switzerland.

Henderson, Y., and Haggard, H.W., 1943. *Noxious gases*, Reinhold Pub. Co.

Lewicki, J.L., Bergfeld, D., Cardellini, C., Chiodini, G., Granieri, D., Varley, N., and Werner, C., 2005. Comparative soil CO_2 flux measurements and geostatistical estimation methods on Masaya volcano, Nicaragua, *Bull. Volcanol.*, 68, 76-90.

Makris, J., Papoulia, J., and Drakatos, G., 2004. Tectonic deformation and microseismicity of the Saronikos Gulf, Greece, *Bul. Seismol. Soc.Am.*, 94(3), 920-929.

Nicholson, K., 1993. *Geothermal fluids*, Springer Verlag, Berlin, 263pp.

Norman, J.M., Garcia, R., and Verma, S.B., 1992. Soil surface CO_2 fluxes and the carbon budget of a grassland, *J. Geophys. Res.*, 97, 18845-18853.

Pecoraino, G., Brusca, L., D'Alessandro, W., Giammanco, S., Inguaggiato, S., and Longo, M., 2005. Total CO_2 output from Ischia Island volcano (Italy). *Geochem. J.* 39, 451-458.

Pe-Piper, G., and Piper, D.J.W., 2002. *The igneous rocks of Greece*, Bornträger, Berlin.

Stothers, R.B., and Rampino, M.R., 1983. Volcanic eruptions in the Mediterranean before A.D. 630 from written and archeological sources, *J. Geophys. Res.*, 88, 6357-6371.

Volti, T.K., 1999. Magnetotelluric measurements on the Methana peninsula (Greece): modeling and interpretation, *Tectonophys.*, 301, 111-132.

Vougioukalakis, G.E., and Fytikas, M., 2005. Volcanic hazards in the Aegean area, relative risk evaluation, monitoring and present state of the active volcanic centers. In Fytikas M. and Vougioukalakis G.E. (eds.) *The south Aegean active volcanic arc – Developments in Volcanology 7*, 161-183.

Witham, C.S., 2005. Volcanic disasters and incidents: A new database, *J. Volcanol. Geotherm. Res.*, 148, 191–233.